HHS Public Access

Author manuscript

*J Control Release*. Author manuscript; available in PMC 2021 August 10.

Published in final edited form as:

*J Control Release*. 2020 August 10; 324: 471–481. doi:10.1016/j.jconrel.2020.05.027.

# One-year Chronic Toxicity Evaluation of Single Dose Intravenously Administered Silica Nanoparticles in Mice and their *Ex vivo* Human Hemocompatibility

**Raziye Mohammadpour**[1], **Darwin L. Cheney**[1], **Jason W. Grunberger**[1,2], **Mostafa Yazdimamaghani**[1,2,#], **Jolanta Jedrzkiewicz**[3], **Kyle J. Isaacson**[1,4], **Marina A. Dobrovolskaia**[5], **Hamidreza Ghandehari**[1,2,4,*]

[1]Utah Center for Nanomedicine, Nano Institute of Utah, University of Utah, Salt Lake City, Utah, United States

[2]Department of Pharmaceutics and Pharmaceutical Chemistry, University of Utah, Salt Lake City, Utah, United States

[3]Department of Pathology, University of Utah, Salt Lake City, Utah, United States

[4]Department of Biomedical Engineering, University of Utah, Salt Lake City, Utah, United States

[5]Nanotechnology Characterization Laboratory, Cancer Research Technology Program, Frederick National Laboratory for Cancer Research sponsored by the National Cancer Institute, Frederick, Maryland, United States

## Abstract

Chronic toxicity evaluations of nanotechnology-based drugs are essential to support initiation of clinical trials. Ideally such evaluations should address the dosing strategy in human applications and provide sufficient information for long-term usage. Herein, we investigated one-year toxicity of non-surface modified silica nanoparticles (SNPs) with variations in size and porosity (Stöber SNPs 46 ± 4.9 and 432.0 ± 18.7 nm and mesoporous SNPs 466.0 ± 86.0 nm) upon single dose intravenous administration to female and male BALB/c mice (10 animal/sex/group) along with their human blood compatibility. Our evidence of clinical observation and blood parameters

*Corresponding author at: 36 S. Wasatch Dr. Salt Lake City, Utah, USA, 84112, hamid.ghandehari@utah.edu, Ph: 801-587-1566, Fax: 801-581-6321.

#Present address: Pharmacoengineering and Molecular Pharmaceutics, Center for Nanotechnology in Drug Delivery, UNC Eshelman School of Pharmacy, Lineberger Comprehensive Cancer Center, UNC School of Medicine, The University of North Carolina at Chapel Hill.

Credit Author Statement

*Raziye Mohammadpour*: Conceptualization, Methodology and formal analysis, Validation, Investigation, Writing Original Draft, Review & Editing; *Darwin L. Cheney*: Methodology, Validation, Investigation, Review & Editing; *Jason W. Grunberger*: Methodology, Validation, Investigation, Review & Editing; *Mostafa Yazdimamaghani*: Methodology, Validation, Investigation, Review & Editing; *Jolanta Jedrzkiewicz*: Investigation, Validation, Review & Editing; *Kyle J. Isaacson*: Methodology, Validation, Investigation, Review & Editing; *Marina A. Dobrovolskaia*, Methodology, Validation, Conceptualization, Review & Editing; *Hamidreza Ghandehari*: Conceptualization, Supervision, Methodology, Validation, Writing, Review & Editing.

Disclosure

No commercial affiliations that might pose a perceived, potential or conflict of interest with this study are available.

showed no significant changes in body weight, cell blood count, nor plasma biomarker indices. No significant changes were noted in post necropsy examination of internal organs and organ-to-body weight ratio. However, microscopic examination revealed significant amount of liver inflammation and aggregates of histiocytes with neutrophils within the spleen suggesting an ongoing or resolving injury. The fast accumulation of these plain SNPs in the liver and spleen upon i.v. administration and the duration needed for their clearance caused these injuries. There were also subtle changes which were attributed to prior infarctions or resolved intravascular thrombosis and included calcifications in pulmonary vessels, focal cardiac fibrosis with calcifications, and focal renal injury. Most of the pathologic lesions were observed when large, non-porous SNPs were administered. Statistically significant chronic toxicity was not observed for the small non-porous particles and for the mesoporous particles. This one-year post-exposure evaluation indicate that female and male BALB/c mice need up to one year to recover from acute tissue toxic effects of silica nanoparticles upon single dose intravenous administration at their 10-day maximum tolerated dose. Further, *ex vivo* testing with human blood and plasma revealed no hemolysis or complement activation following incubation with these silica nanoparticles. These results can inform the potential utility of silica nanoparticles in biomedical applications such as controlled drug delivery where intravenous injection of the particles is intended.

## Graphical Abstract

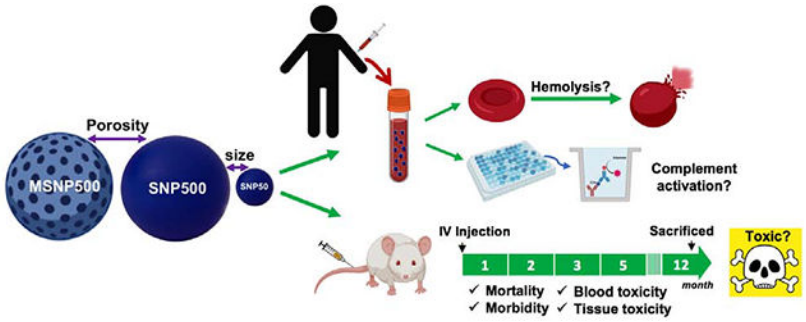


### Keywords

Chronic toxicity; Nanotoxicology; Silica nanoparticles; Porosity; Hemocompatibility; Complement; One-year; BALB/c mice

## Introduction

The majority of research in nanotoxicology has been focused on short term toxicity evaluation of nanoparticles.[1–4] Long-term exposure to nanoparticles can have adverse consequences that may not be observed in acute toxicity studies. When nanoparticles are administered *in vivo*, based on their body circulation time, biodistribution and the time needed for their degradation and elimination from the body, persistence of adverse effects can influence their long-term safety profile. For example, it has been shown that gold content is still detectable in the urine and blood of subjects three months after single dose inhalation of 5 and 30 nm gold nanoparticles.[5] It is clear that a specific dose of the drug might decrease the disease symptoms without major toxicity in a short period of time, but

adverse effects associated with chronic exposure is one of the main reasons for withdrawal of pharmaceuticals from the market.[6] Regulatory guidelines outline safety evaluation of medicinal products from 6 up to 12 months, based on duration and route of exposure and type of animal, before approval and marketing.[7, 8] For example, chronic toxicity testing on juvenile animals should address the carcinogenicity and developmental concerns of drug products before pediatric clinical trials.[8] Long-term or delayed toxicities such as genotoxicity, developmental toxicity, and carcinogenesis might take months to years to appear. Potential carcinogenicity of organic and inorganic nanoparticles such as carbon nanotubes, titanium oxide and crystalline silica nanoparticles over time has been reported.[9] For example, Lu X. *et al.* have reported 120 days after single dose pulmonary exposure to multi-walled carbon nanotubes induced significant chronic inflammation and enhanced breast tumor angiogenesis leading to lung metastasis in female BALB/c mice.[10]

Inorganic nanoparticles have been used for different biomedical applications including controlled release and *in vivo* imaging.[11–16] The subchronic and chronic *in vivo* toxicity of inorganic nanoparticles have been reviewed recently.[17] It has been reported that persistent exposure or long time post-exposure to inorganic nanoparticles correlate with inflammation, fibrosis,[18–23] immunotoxicity,[24] neurotoxicity,[25–27] carcinogenesis,[28, 29] and vascular diseases,[5] in animal and human models. The potential long-term toxicity of inorganic nanoparticles can be related to a number of factors including their physiochemical properties, route, dose and frequency of administration, the animal species in which the studies are conducted, and sex of the animals.[17]

Silica-based nanoparticles are inorganic nanoparticles with potential in biomedical applications such as controlled drug delivery and as imaging agents or theranostics.[14, 30, 31] Various compositions of Cornell prime dots (C'-dots) for example are in clinical trials for the diagnosis of brain, breast, head and neck and colorectal cancer.[32, 33] Targeted SNPs (fluorescent cRGDY-PEG-Cy5.5-C dots) have been used for real-time image-guided intraoperative mapping of nodal metastasis. $^{89}$Zr-DFO-cRGDY-PEG-Cy5-C' dots and $^{64}$CuNOTA-PSMAi-PEG-Cy5.5-C' dots have also been investigated in human clinical trials for imaging of brain and prostate cancers, respectively. There have been efforts for using $^{124}$Ilabeled cRGDY silica nanomolecular particle tracers for imaging of patients with melanoma and malignant brain tumors as well. Other ongoing clinical trials where silica nanoparticles are used include treatment of periodontal intrabony defects, Ridge deficiency, dental fluorosis, tooth discoloration, and acute diarrhea.[34, 35] Despite these advances, there is limited information on acute (less than 24 hours), subacute (within one month), subchronic (within 1–3 months) and chronic (after 3 or more months) toxicity of silica nanoparticles as a function of their physicochemical properties.[17] The *in vivo* subacute toxicities of silica nanostructures including 14 days toxicity study of hollow mesoporous silica nanoparticles (HMSNP),[36] and non-porous and mesoporous SNPs with different sizes and aspect ratios[37–40] upon single and repeated dose intravenous administration have been reported. Subchronic toxicity of different silica nanoparticles 45 days,[41] 56 days,[42] and up to 60 days[43] upon IV injection has also been evaluated. There have been some efforts to understand the subchronic (28–84 days) safety of colloidal and mesoporous[44] and synthetic amorphous silica nanoparticles[22] upon intraperitoneal[22] and oral[44] administrations as well. Altogether, these reports indicate that based on the type, size, and porosity of silica

nanoparticles, and clinical usage design (the dose, route, frequency, and duration of administration), these nanoparticles manifest different subchronic toxicity patterns.

To date, the majority of long-term toxicity studies on inorganic nanoparticles have been performed for the duration of up to 13–14 weeks after administration. There are a few studies which extend evaluation to more than 90-days and even fewer that are extended up to one-year.[45] Kolonsjaj and coworkers showed that the gold part of gold/iron oxide nanoheterostructures can persist in female C57/Bl6 mice liver and spleen up to one year upon intravenous (IV) administration.[46] The coating of these nanoparticles influences their biodistribution, degradation and clearance, where amphiphilic polymer (poly(maleic anhydride alt-1-octadecene))-coated gold/iron oxide nanoparticles showed lower degradability compared to poly(ethylene glycol) (PEG)-coated ones.[46] Clearly there continues to be a critical need to understand the chronic toxicity of inorganic nanoparticles including silica nanoparticles.

Previously, we investigated the effects of porosity, size, geometry and surface characteristics of amorphous silica nanoparticles on their *in vivo* biodistribution and short-term toxicity in CD-1 mice upon single dose IV injection, as well as on *in vitro* toxicity in mouse macrophage cell lines.[37, 38, 47–53] Recently, we reported acute and subchronic (10 days, 60 days, and 180 days) toxicity of silica nanoparticles with different sizes and porosities (SNPs50, SNP500, MSNP500) upon single dose IV administration in male and female BALB/c mice.[4] Our data showed size-, porosity-, and sex-dependent acute toxicity of SNPs where smaller and porous nanoparticles had lower maximum tolerated dose (MTD) and male mice showed less tolerance (lower MTD) to injected mesoporous SNPs compared to nonporous particles of the same size.[4] In our studies, we found silica content in the mouse tissues (liver, spleen, and rarely lung) up to 60 days post single dose IV injection. This accumulation caused reticuloendothelial organ injuries where most of the lesions were a result of obstruction of blood capillaries after acute exposure to SNPs upon IV administration and then the body's effort to heal the damaged tissue ensued which resulted in subchronic inflammation.[4] In this manuscript, we report the results of the extension of this study on the same particles to one-year. The effect of SNP size and porosity upon single dose IV injection to female and male BALB/c mice at their 10-day maximum tolerated dose over one year is reported.

Due to their size, IV administration of drug products containing nanomaterials is common.[54] Understanding nanoparticle-blood interaction is critical before a meaningful translation for clinical practice. Numerous nanoparticles including silica nanoparticles have been found to have concentration-, size- and geometry-dependent hemocompatibility.[55] Here, we have further evaluated the hemolytic and complement activation of silica nanoparticles in human blood as a function of aforementioned physicochemical properties.

## Materials and Methods

### 1.1. Silica nanoparticle synthesis and physiochemical characterization

SNPs were synthesized using the Stöber method and characterized as described previously.[4, 47] In brief, size and morphology were determined by Transmission Electron Microscopy

(TEM) ) with a JEOL JEM 1400 microscope (JEOL Ltd., Tokyo, Japan) operating at 120 kV. Hydrodynamic size and zeta potential were measured by dynamic light scattering (DLS) using a Zetasizer Nano ZS (Malvern Instruments Ltd., Worcestershire, U.K.). The nanoparticles were determined to be clinically endotoxin free through photometric quantification of endotoxin lipopolysaccharide (LPS) by using Pierce™ Chromogenic Endotoxin Quant Kit (Thermo Scientific Inc., Waltham, MA, U.S.A.). We used the exact same nanoparticles for this study as we did for the acute and subchronic toxicity studies reported previously.[4] These were three different silica nanoparticles in two sizes, namely, Stöber silica nanoparticles (432 ± 18.7 nm (Stöber SNPs500) and 46 ± 4.9 nm (Stöber SNPs50)), and mesoporous silica nanoparticles (466 ± 86 nm (MSNPs500)) comparable in size to the larger Stöber SNPs (Figure S1 and Table S1).

### 1.2. Animals and nanoparticle administration

All animal procedures were approved by The University of Utah Institutional Animal Care and Use Committee (IACUC). 43–49 days old female and male inbred immune intact BALB/c mice were obtained from Charles River Laboratories (strain code #28). The animal groups (5 mice/cage) were acclimated to 12 h light/dark cycle with free access to water and food under 20% humidity and 72–74°F temperature for two weeks prior to injection. The cages were randomly assigned to control and treatment groups with 10 animal/group/sex. Mice were dosed with freshly prepared SNPs in 0.9% saline solution through tail vein intravenous administration at their 10-day MTD (100 mg $kg^{-1}$ for SNP50 and MSNP500 and 300 mg $kg^{-1}$ for SNP500)(Table S1)[4] in 150 μL suspension (Table S2) using 28G syringes (BD, VWR, Radnor, PA). It should be mentioned that MTD for MSNPs were different in both sexes (100 mg $kg^{-1}$ in female and 40 mg $kg^{-1}$ in male). Same dose of MSNPs (100 mg $kg^{-1}$) was injected to both female and male mice to see the long-term effect at equal dose (Table S2). The general behavior and body weight changes of mice were monitored and recorded daily up to 10 days, 2 times/week up to two months, weekly up to six months, and once per month until one year.

### 1.3. Necropsy and organ weight measurement

The animals were sacrificed one-year after administration by exsanguination following inhalation of 5% isoflurane using vaporizer (Vetequip, CA, USA). Following necropsy, main vital organs (liver, lung, spleen, brain, kidney, heart, stomach, intestine and reproductive organs) were extracted and weighted freshly using Mettler-Toledo XP204 balance (Columbus, OH, USA). The collected tissues were preserved in 10% neutral buffered formalin (VWR, Radnor, PA) for further histological examination.

### 1.4. Hematology and blood chemistry

Upon animal anesthesia, blood was collected into sodium heparin and K2- EDTA (3.6 mg) tubes (BD, VWR, PA, USA) from heart using 31 G syringes. Cell blood count and hematology parameters were determined by Heska CBC-HT5 instrument (Loveland, CO, USA). Plasma of the blood samples was obtained by centrifuging at 3,000 Xg for 15 min and the blood chemistry parameters were determined using a Heska DRI-CHEM veterinary blood chemistry analyzer (Loveland, CO, USA).

### 1.5. Histopathological examination

The dissected organs during necropsy including lung, liver, brain, heart, intestine and genitourinary organs, were fixed in formalin for three days and then transferred to an ethanol solution (70%). Tissue samples were submitted in tissue embedding cassettes (Simport, Canada), processed by Tissue-Tek VIP 6 Vacuum Infiltration Processor (Sakura Finetek, CA, USA) at ARUP Laboratories (Salt Lake City, Utah). The sections were obtained from the prepared tissue blocks using Leica Microm RM55 Rotary Microtome (IL, USA) and placed on glass slides, later stained with Hematoxylin and Eosin on Tissue-Tek Prisma Automated Slide Stainer (Sakura Finetek, CA, USA). Slides were scanned with Aperio digital pathology slide scanner (Leica Biosystems, IL, USA) and analyzed with Image Scope software (Leica Biosystems, IL, USA).

### 1.6. Blood collection and plasma preparation

The human blood samples were used based on approved procedures of The University of Utah Institutional Review Board (IRB). Venous blood of eight healthy volunteers who were medication- (non-prescribed and birth control medications not included) and alcohol-free for 72 hours was collected following the NCI Nanotechnology Characterization Laboratory (NCL) protocol.[56] Both ABO and Rh type were determined for each donor using an Eldoncard blood typing kit (Eldon Biological, Denmark) and compatible plasma was pooled. The first 10 mL of blood was discarded.

Complete blood count (CBC) analysis of whole blood was subsequently preformed using a Heska Element HT5 (Heska Corp., Loveland, CO, U.S.A.) to evaluate overall health of each donor. SNP concentrations for all blood studies were selected based on relevant injected doses in mice and theoretical plasma concentrations in human doses as described previously.[57] The samples tested were SNPs500, MSNPs500, SNPs50 at final concentrations of 0.005, 0.05, 0.1, and 0.3 mg $mL^{-1}$ in 0.9% normal saline.

### 1.7. Hemolysis assay

SNPs were mixed with diluted whole blood (contain 10 ± 2 mg $mL^{-1}$ total blood hemoglobin) and incubated at 37°C for 3 hours. Stable form of hemoglobin, CMH reagent (Drabkin's solution containing cyanide) was detected spectrophotometrically at 540nm using Spectra Max M2 spectrophotometer (Molecular Devices, Sunnyvale, CA). The amount of released hemoglobin upon hemolysis was analyzed by using a calibration curve of Drabkin's reagent and Brij (Sigma Aldrich, MO, USA) and quality controls from commercially available human hemoglobin (Sigma Aldrich, MO, USA) as described before.[58, 59] Triton X-100 (Acros Organic, NJ, USA ) was used as a positive control.

### 1.8. Complement activation assay

Plasma was prepared by centrifugation of fresh whole blood at 2500 X*g* for 10 minutes. Equal volumes of plasma, Veronal buffer (Boston Bioproducts, MA, USA) and the samples were mixed together and incubated at 37°C for 30 min. The samples were stored in −80°C before use. The amount of iC3b was detected by Quidel iC3b ELISA Immunoassay (EIA) MicroVue Complement kit (Thermo-Scientific, Pittsburgh, PA) following manufacturer's

protocol. Cremophor (EMD Millipore, MA, USA) and 0.9% saline solution were used as positive and negative controls, respectively.

### 1.9. Statistical analysis

GraphPad Prism 8 software (CA, USA) was used to perform statistical analysis. Results are presented as mean ± standard deviation. The difference between values was considered significant at the level of $p < 0.05$.

## Results

During the one-year study, all the mice showed no statistically significant difference in growth rate from the saline injected control group (Figure 1). The female and male mice had some loss of hair on the muzzle, neck and two sides of their body as described below. Three out of 10 males in the control group, 5 out of 10 males that received Stöber SNPs50, and 2 out of 10 males in both Stöber SNPs500 and MSNPs500 group showed hair loss. In females, one animal in the control group and four out of 10 in both Stöber SNPs500 and Stöber SNPs50 groups showed hair loss. The earliest time for the hair loss occurred on day 49 after injection and continued for several weeks until hair grew back. Some clinical morbidity including shortness of breath and weakness in back hind leg was observed in two female mice that received Stöber SNPs500 (on day 5 and day 301) which lasted for a week. In the same group, one other animal lost weight on day 301 and was found dead 364 days after injection. A female animal in the control group also became sick on day 329 with signs of loss of weight, rigid tail, shortness of breath and black eye and veins, and died on day 339. In addition to these three animals, one male in control group was found dead on day 211 without any clinical abnormality. Thus, 4 out of 80 mice died during the one-year study (Figure 1, inset).

At the end time point, the surviving animals were sacrificed. No gross tissue injuries were found in any injected female and male mice. The weight to body ratio percent of various vital organs were not significantly different in comparison to saline injected control groups as shown in Figure 2.

The different blood cells were counted in blood withdrawn from heart of sacrificed animals. As Figure 3 shows, the number of platelets, red blood cells, the different types of white blood cells (basophil, lymphocyte, eosinophil, monocyte, neutrophil), other blood parameters such as hemoglobin, hematocrit, red blood cell distribution, mean cell hemoglobin concentration and mean cell volume in SNP administered animals were the same as those of the control group and all were in the normal range.

The levels of glucose, total protein, aspartate amino transferase (AST), alkaline phosphatase (ALP), alanine aminotransferase (ALT), and blood urea nitrogen (BUN) were measured in the surviving one-year animals. Female and male BALB/c mice that received Stöber SNPs500, SNPs50 and MSNPs500 had normal levels of indicated plasma biochemical indices (Figure 4).

Histology evaluation showed evidence of tissue injury one-year after SNPs IV single administration. One male and one female animal that received SNPs500 and SNP50, respectively, showed foci of scarring within the heart, pericardial calcifications or myocardial calcification (Figure 5A). Two female mice previously injected with SNPs500 and SNPs50 had focal calcifications in pulmonary vasculature (Figure 5B). Examined kidneys of three male mice that received large SNPs had mild chronic lymphocytic inflammation within the interstitial space along with focal tubular injury (Figure C and D) and luminal casts composed of white blood cells debris. Notably, there were also two male mice with focal renal interstitial fibrosis and hemosiderin deposition in the control group; however, neither tubular injury nor ongoing parenchymal damage was observed in those animals. Several lesions were observed in the liver tissue microscopically. There was one animal with subcapsular hepatic fibrosis and calcification, previously injected with SNPs50. Seven of the twelve treated animals (58%) showed inflammation within the liver tissue consisting of scattered aggregates of mostly lymphocytes with admixed histocytes or pigment laden macrophages (Figure 5F). This inflammation was largely located within the hepatic lobules or perivascular spaces. There was also minimal to mild macrovesicular steatosis (1% - 15%) (Figure 5E) noted in multiple animals from both treated and control groups. One saline injected female mouse showed significant (90%) microvesicular steatosis (Figure 5G), which was an unexpected finding not seen in other samples. Focal hemosiderin deposition within the spleen was noted in multiple animals from both the treated and control groups (Figure 5J). The fast accumulation of these plain SNPs in the liver and spleen upon i.v. administration and the duration needed for the clearance of the particles, probably caused these injuries. Four animals injected with SNPs500 showed aggregates of histocytes with neutrophils or necrosis within the splenic white pulp (Figure 5I). Brain and reproductive organs of all studied animals (4 animals for each treatment group) did not show remarkable pathology alterations. The observed pathologic lesions were mostly in the animals that were injected with large, non-porous SNPs compared to small non-porous SNPs and mesoporous SNPs.

To further understand the potential mechanisms underlying silica nanoparticle effects on blood components, hemolysis and complement activation were evaluated. Since in vitro analysis of rodents' blood is known to be insensitive to these toxicities, we used human blood. This choice is supported by the literature reports suggesting that human blood assays correlate with clinical findings in patients and represent a sensitive model as opposed to in vitro rat or mouse blood assays (reviewed in [57]). Furthermore, the complement activation is known to underlie both short-term (e.g., anaphylactoid reactions) and long-term (e.g., the induction of adaptive immunity through activation of T- and B-cell responses) effects.[60, 61] Figure 6 shows relative hemolytic activity and activation of complement pathway in the presence of SNPs500, SNPs50 and MSNPs500 at the different tested concentrations. Although, the assay positive control, Triton X-100, induced about 100% hemolysis, we did not see any significant hemolysis in any of the SNP samples (0.05 – 0.3 mg $mL^{-1}$) compared to negative control (0.9% saline solution). We also observed that none of the tested samples promoted complement when normalized to saline control.

## Discussion

There continues to be a growing interest in detailed evaluation of safety of inorganic nanoparticles. Despite significant studies on *in vitro* and *in vivo* acute toxicity of inorganic nanoparticles, the long-term monitoring of potential risk of these materials is limited. Having the knowledge of what might happen over months after nanoparticle administration, relative to dose and physiochemical properties, helps the medical community to be alert, predict and potentially prevent and cure the side effects resulting from intended or unintended exposure to inorganic nanoparticles. In this study, we examined the toxicity of silica nanoparticles with different sizes and porosities one-year post single dose intravenous injection in two sexes of BALB/c mice. Our findings show that exposures to different silica nanoparticles (Stöber SNPs50 and SNPs500, and MSNPs500) were tolerated without statistically significant changes in morbidity and body weight changes (Figure 1) and hematological profile including cell blood count and blood biomarker indices (Figures 3 and 4). Two female mice that were injected with non-porous SNPs500, showed clinically significant symptoms 10 months after IV injection at MTD (300 mg $kg^{-1}$). The observed clinical abnormalities (e.g., weakness in the back hind leg and weight loss) were the same as those we observed upon injection of the same particles at high dose (more than MTD) during 10-day toxicity study.[4] This mortality is not significant since two animals (one female and one male) from control group died during the year as well. Hair and whisker loss were observed in all groups during the one-year study for both female and male BALB/c mice. It has been reported that barbering, which is a social behavior of fur/whisker trimming, is a common behavior in laboratory rodent animals (2.5–4 months old).[62–64] We believe this observation is related to the aging of the animals or long-term group housing. Further long-term phenotype evaluation of BALB/c mice is needed to address this issue.

Previously, our acute toxicity study revealed that brain, heart, lung, liver, kidney and spleen were the target organs upon IV bolus administration of the same silica nanoparticles (SNPs50 and SNPs500, and MSNPs500) to female and male BALB/c mice at the doses greater than 10-day MTD.[4] Further, subchronic toxicity evaluation of the same particles demonstrated that even though the silica nanoparticles were cleared from the reticuloendothelial organs (liver, spleen, and lung) during 60 to 180 days after single IV injection (Figure S2), still there were increased inflammatory signals (up to 60 days) and significant lesions in liver, lung, and spleen (up to 180 days) after injection at MTD.[4] The representative one-year histopathological examination on the same particles showed a few animals still had clinically significant pathologic lesions without organ weight changes (Figures 2 and 5). There were calcifications within the pulmonary vessels observed in two animals (female SNPs500, male SNPs50) from our cohort. These changes are likely to represent sites of prior intravascular thrombi that have since resorbed (Figure 5). Vascular calcifications are known to occur in pulmonary thrombosis or inflammation.[65, 66] Proinflammatory cytokines, have been observed upon subchronic exposure to SNPs,[4] and macrophage release products that promote deposition of calcium in vessels.[66] Vascular insufficiency is also a common cause of chronic renal and heart failure.[67] There were two female animals receiving SNPs500 that had kidneys showing interstitial inflammation, tubular injury, and luminal casts one-year after injection. There were also two animals

showing fibrosis and calcifications within the heart after one year (Figure 5). We hypothesize that these changes have resulted from compromised vascular supply or outflow, through particles induced obstruction. More experimental evidence is needed to confirm this hypothesis.

Liver is one of the organs where nanoparticles are known to accumulate following IV administration.[68] Two female mice which received large non-porous SNPs500 in our study showed numerous aggregates of lymphocytes with admixed histocytes within their livers. The degree of inflammation varied but was noted in up to 58% of all treated animals. There was no significant liver fibrosis or cirrhosis noted on H and E stained slides apart from one sample (female who recovered from SNP50) which showed focal fibrosis with calcifications limited to subcapsular region (Figure 5). Overall, data suggest that the observed inflammation likely resulted from the remote administration of nanoparticles because similar changes were not seen in the control animals. Inflammatory infiltrates may take time to resolve completely. Therefore, the observed inflammation could indicate resolving or ongoing injury as well. Another microscopic alteration observed in multiple liver samples was macrovesicular steatosis involving 1% to 15% of all hepatocytes, minimal to mild in severity. These changes were observed in the treated animals as well as the control groups. Therefore, it is difficult to be certain about causation. However, diet, amount of exercise and body mass index influences accumulation of fat in the liver. Drugs and toxins are also known to cause liver steatosis clinicaly.[69] Therefore the association between steatosis and nanoparticles cannot be completely excluded. Of note is that there was one female from the control group that showed more than 90% microvesicular steatosis. This was an unexpected finding not seen in other control samples. Microvesicular steatosis as seen in this case, may have been influenced by diet or other process causing deranged mitochondrial beta oxidation.[70, 71] Commonly considered etiologies include metabolic diseases and drug/toxin effects. These latter causes are unlikely because metabolic diseases are very rare in experimental animals, there was no uncontrolled drug or toxin administration, and the mice were housed with the same sex animals precluding pregnancy.

Four animals injected with SNPs500 (two females and two males) showed accumulation of histocytes with neutrophils or necrosis within the splenic white pulp, which was interpreted to represent splenic macrophages taking up SNPs prior to further clearance or granulomatous drug reaction. Another lesion found in the spleen was focal hemosiderin deposition which was observed in treated animals (all males and also in females (SNPs500 injected)) and samples from control groups, that could be age associated change, unrelated to nanoparticles.

Overall, it can be concluded that most of the pathologic lesions were observed in the animals that were injected with large, non-porous SNPs. The MTD of these SNPs was higher, which means more SNPs500 (300 mg $kg^{-1}$) were injected into the animals compared to the other studied SNPs (100 mg $kg^{-1}$). Thus, the body needed more time to clear and heal from the injected silica. Second, we have shown that porosity of silica nanoparticles changes their *in vitro* degradation and excretion from the body.[48] MSNPs (100 nm) were shown to degrade much faster than the same size Stöber SNPs in different simulated body fluids and in RAW 246.7 macrophages.[48] In addition, 28-day excretion study of MSNPs showed 53% of silicon

content in the urine compared to about 27% in non-porous SNPs following IV administration to female CD-1 mice at the same dose.[48] We have shown MSNPs500 degrade 50–80% in simulated lysosomal fluid (pH 4.5), simulated intestinal fluid (pH 6.5), simulated body fluid (pH 7.4), and in deionized (DI) water pH 6 after 28 days. In addition to surface area and porosity, it has been shown that MSNP's hydrolytic susceptibility and stability is dependent on the silica network connectivity and degree of condensation. Möller and Bein observed that synthesis conditions and particle composition determine degradability by varying the degree of condensation.[70] MSNPs synthesized under basic conditions resulted in lower network connectivity and more rapid dissolution kinetics when compared to MSNPs synthesized in acidic conditions.[72] Therefore, faster clearance of MSNPs along with their lower dose of injection may be the reason for the observed safety profile of these NPs and delayed tissue repair for Stöber SNPs in our one-year study. The nanoparticle size may influence the long-term toxicity in that smaller porous SNPs may have different behavior compared to nonporous SNPs; such comparison needs to be investigated in the future within the context of specific applications

One concern regarding intravenously administered nanoparticles is the lysis of red blood cells and immunotoxicity upon interaction with blood cells and plasma proteins.[73] Experiments conducted in this study did not reveal any detectible hemolysis upon three hours incubation of fresh human whole blood with SNPs50 and SNPs500, and MSNPs500 (Figure 6a). Although, earlier studies suggested SNPs have hemolytic activity which correlate with their porosity and geometry.[49] The data here emphasize that this effect is associated with the concentration of nanoparticles, number of exposed red blood cells, and incubation condition. Also, it has been reported that opsonization of complement protein on the surface of nanoparticles causes immunogenicity[74, 75] which is physiochemical properties-dependent.[56, 76, 77] Human complement component proteins have been found on the surface of silica nanoparticles with various sizes ( 20, 30, 100 nm) where the size was critical for the type and amount of this protein corona.[78] Complement proteins including complement C4, C4 isoform X2, and complement factor I, H, and B precursor, are dominant in the protein corona around SNPs50, SNPs500 and MSNP500 nanoparticles.[47] Our data here revealed, however, that none of the studied SNPs at the indicated concentrations (0.005–0.3 mg $mL^{-1}$) promote complement activation through increasing iC3b protein level (Figure 6b). Previous studies with silica nano- and microparticles (180 nm and more than 1μm) have indicated that they do not activate intracellular complement.[76] These data show that the relevant human maximum tolerated dose of SNPs does not induce hemolysis and immunotoxicity upon activation of complement pathway in human blood. Further studies on platelet aggregation and plasma coagulation in the presence of SNPs at MTD are needed to establish the hemocompatibility of these nanoparticles.

Safety evaluation of silica nanoparticles with variations in physicochemical properties following intravenous administration has been reported. Liu *et al.* reported that 110 nm hollow mesoporous SNPs accumulated in liver and the particles had LC50 at the dose more than 1 g $kg^{-1}$ in ICR mice upon single dose intravenous administration, and that daily repeated IV administration for 14 days at 20–80 mg $kg^{-1}$ of the same particles did not result in death.[36] It has been reported that male BALB/c mice tolerated different doses (1–300 mg $kg^{-1}$) of single intravenously administered SNPs (150 nm) for 14 days without any

significant blood and tissue toxic effects.[39] In addition, 45-day subchronic pulmonary inflammation with accumulation of collagen was observed in male ICR mice upon receiving 20 mg $kg^{-1}$ amorphous SNPs (62 nm) through tail vein injection once per three days.[41] Eight-week toxicity testing of 10 nm negatively charged SNPs (5 mg $kg^{-1}$) upon weekly IV administration to female BALB/c mice demonstrated an increase in pro-inflammatory cytokines in serum along with liver inflammation.[42] Subchronic hepatotoxicity of different sizes of silica nanoparticles (20, 70, 80, 300 and 1000 nm) was also reported upon IV injection.[79, 80] These studies clearly establish the fact that short- and long-term toxicity of SNPs upon IV injection depends on their physiochemical properties, dose and frequency of administration. The detailed mechanisms of the toxicity of SNPs needs to be established. Our studies on acute and subchronic[4] and this report of chronic toxicity of the same silica nanoparticles as a function of size and porosity on female and male BALB/c mice suggest the possible mechanisms of toxicity and the ensuing healing outcomes that are summarized in Figure 7.

Single dose IV injection of silica nanoparticles in female and male BALB/c mice, causes blood vein obstruction which could be caused by aggregation upon injection. Infarction and thrombosis then ensue especially in the main accumulated organs, lung, spleen and liver. The tissue lesions remained sub-chronical (60–180 days upon injections) with increasing inflammation and aggregation of macrophages and neutrophils, and calcification to heal the injured organs.[4] On the other hand, acute and subchronic blood toxicity which appeared to decrease WBC happens upon administration of silica nanoparticles which might be a result of direct toxicity of particles to macrophages and possibly reversible bone marrow suppression which continued up to 60 days after injection (Figure S3). Therefore, Stöber SNPs 46 ± 4.9, Stöber SNPs 432.0 ± 18.7 nm, and mesoporous SNPs 466.0 ± 86.0 nm at their 10-day maximum tolerated doses cause acute and slight subchronic toxicity in female and male BALB/c mice. The animals needed six months to one year to recover from induced acute toxicity of silica nanoparticles upon single dose intravenous administration. This recovery time was porosity-and size-dependent. Most of the lesions we observed upon IV injection were the result of blood obstruction probably due to the aggregation of SNPs under physiological conditions. Therefore, stabilizing silica NPs to decrease aggregation/agglomeration such as surface functionalization with poly(ethylene glycol)[81] in addition to decreasing the dose of injection and increasing the dosing frequency might potentially reduce the long-term tissue toxic effects of these nanoparticles.

It is clear that the toxicity of SNPs relates to the amount of delivered SNPs that in turn, depends on the cargo to be delivered, the loading capacity of the carrier, and frequency of administration. The size, charge and porosity of MSNPs defines their loading capacity for different applications such as cancer therapy.[82] Shen *et al.*, for example, found the maximum loading capacity of 120 nm MSNPs with pore volume of 0.32 $cm^3$ $g^{-1}$ to be 306 mg doxorubicin (DOX) per 1g MSNPs.[83] The mass of DOX dose for a standard dose of clinical treatment (75 mg $m^{-2}$ IV q21 Days) would be 136.88 mg in the average human adult (weight of 70 kg and height of 1.72 m). Therefore, based on the reported loading capacity of MSNPs,[83] the mass of MSNPs needed for a single injection would be 0.45 g. The relevant MTD of MSNP500 we observed was 0.57 g in humans. Thus, a single dose administration of DOX loaded MSNP500 will be close to MTD and may result in acute and subchronic

toxicity.[4] However 21 days repeated dose administration might cause significant silica related toxicities since this duration is not enough for recovery. However, the theoretical loading capacity of MSNP500 might be less than MSNP 120 nm due to smaller surface area. Other approaches such as use of hollow mesoporous nanoparticles can reduce the amount of silica to be administered while maximizing loading capacity. Having the knowledge of the long-term effects of SNPs at a specific dose upon IV injection along with detailed understanding of their degradation and elimination profile, dosing frequency, drug potency and other parameters can inform the rational design of the type and dose of SNPs for specific controlled release applications. Our data clearly shows that the long-term toxicity of silica nanoparticles is physiochemical properties dependent. Any changes in the surface functionalization of these nanoparticles such as attachment of poly(ethylene glycol) will likely change the long-term toxicity profile as well. The data reported here emphasizes the importance of long-term toxicity evaluation of nanoparticles which needs to be done on a case by case basis depending on the context in which they are being used.

## Conclusions

Altogether, our one-year toxicity evaluation of SNPs indicates that non-surface modified Stöber SNPs 46 ± 4.9 nm, Stöber SNPs 432.0 ± 18.7 nm, and mesoporous SNPs 466.0 ± 86.0 nm do not cause chronic toxicity in female and male BALB/c mice following single dose intravenous bolus administration at their 10-day maximum tolerated dose. We observed only a few animals with microscopic lesions in liver, kidney, spleen or lungs which could have resulted from previous intravascular thrombosis, or focal resolving or ongoing inflammatory response. The observed pathologic lesions were mostly in the animals that were injected with large, non-porous SNPs. No statistically significant chronic toxicity was observed for the small non-porous SNPs and for the MSNPs. Relevant MTD of small, large and mesoporous SNPs did not induce hemolysis or activate the complement pathway in human blood sample *ex vivo*. This study provides information for safe and effective design of SNPs in controlled delivery applications. It must be stated that depending on dose, frequency of administration and physicochemical properties of SNPs the toxicity profile of SNPs will change.

## Supplementary Material

Refer to Web version on PubMed Central for supplementary material.

## Acknowledgment

Funding for this study was provided by the National Institute of Environmental Health Sciences of the National Institutes of Health under award No. R01ES024681 as well as the ALSAM Foundation. The H & E staining was conducted with the assistance from the biorepository and molecular pathology shared resources supported by the grant awarded to the Huntsman Cancer Institute by the National Cancer Institute of the National Institutes of Health under CCSG grant No. CA042014-31. The authors also acknowledge the use of The University of Utah shared facilities of Micron Microscopy and the University of Utah USTAR shared facilities supported in part by the MRSEC Program of the National Science Foundation under award No. DMR-1121252. Biorender.com (Toronto, Ontario) tool was used to create the graphical abstract. We also would like to Acknowledge Maria Reyes, for assisting in blood draw from volunteers. The study was supported in part (to M.A.D.) by federal funds from the National Cancer Institute, National Institutes of Health, under contract HHSN261200800001E and 75N91019D00024. The content of this publication does not necessarily reflect the views or policies of the

Department of Health and Human Services, nor does mention of trade names, commercial products, or organizations imply endorsement by the U.S. Government.

## Abbreviations

| | |
|---|---|
| **SNPs** | silica nanoparticles |
| **MSNPs** | mesoporous silica nanoparticles |
| **TEM** | transmission electron microscopy |
| **MTD** | maximum tolerated dose |
| **IV** | ntravenous |
| **AST** | aspartate amino transferase |
| **ALP** | alkaline phosphatase |
| **ALT** | alanine aminotransferase |
| **BUN** | blood urea nitrogen |
| **BN** | brain |
| **LN** | lung |
| **RO** | reproductive organ |
| **HT** | heart |
| **SP** | spleen |
| **ST** | stomach |
| **IN** | intestine |
| **KD** | kidney |
| **C'-dots** | Cornell prime dots |
| **ZnO** | Zinc oxide |
| **LC 50** | lethal dose 50% |
| **LPS** | Lipopolysaccharide |
| **EIA** | Elisa immunoassay |
| **Dox** | doxorubicin |
| **PEG** | poly(ethylene glycol) |

## References


1. Munger MA; Radwanski P; Hadlock GC; Stoddard G; Shaaban A; Falconer J; Grainger DW; Deering-Rice CE, In vivo human time-exposure study of orally dosed commercial silver nanoparticles. Nanomedicine: Nanotechnology, Biology and Medicine 2014, 10 (1), 1–9.
2. Li X; Wang L; Fan Y; Feng Q; Cui F. z., Biocompatibility and toxicity of nanoparticles and nanotubes. Journal of Nanomaterials 2012, 2012, 6.
3. Bahadar H; Maqbool F; Niaz K; Abdollahi M, Toxicity of nanoparticles and an overview of current experimental models. Iranian biomedical journal 2016, 20 (1), 1. [PubMed: 26286636]
4. Mohammadpour R; Yazdimamaghani M; Cheney DL; Jedrzkiewicz J; Ghandehari H, Subchronic toxicity of silica nanoparticles as a function of size and porosity. Journal of Controlled Release 2019, 304, 216–232. [PubMed: 31047961]
5. Miller MR; Raftis JB; Langrish JP; McLean SG; Samutrtai P; Connell SP; Wilson S; Vesey AT; Fokkens PH; Boere AJF, Inhaled nanoparticles accumulate at sites of vascular disease. ACS nano 2017, 11 (5), 4542–4552. [PubMed: 28443337]
6. Siramshetty VB; Nickel J; Omieczynski C; Gohlke B-O; Drwal MN; Preissner R, WITHDRAWN—a resource for withdrawn and discontinued drugs. Nucleic acids research 2015, 44 (D1), D1080–D1086. [PubMed: 26553801]
7. Van Cauteren H; Bentley P; Bode G; Cordier A; Coussement W; Heining P; Sims J, The industry view on long-term toxicology testing in drug development of human pharmaceuticals. Pharmacology & toxicology 2000, 86, 1–5. [PubMed: 10905744]
8. U.S. Department of Health and Human Services Food and Drug Administration, C. f. D. E. a. R. C., Center for Biologics Evaluation and Research (CBER), Guidance for industry, M3(R2) nonclinical safety studies for the conduct of human clinical trials and marketing authorization for pharmaceuticals. 2010; Vol. Revision 1.
9. Becker H; Herzberg F; Schulte A; Kolossa-Gehring M, The carcinogenic potential of nanomaterials, their release from products and options for regulating them. International journal of hygiene and environmental health 2011, 214 (3), 231–238. [PubMed: 21168363]
10. Lu X; Zhu Y; Bai R; Wu Z; Qian W; Yang L; Cai R; Yan H; Li T; Pandey V, Long-term pulmonary exposure to multi-walled carbon nanotubes promotes breast cancer metastatic cascades. Nature Nanotechnology 2019, 1.
11. Paul W; Sharma CP, Inorganic nanoparticles for targeted drug delivery In Biointegration of Medical Implant Materials, Elsevier: 2020; pp 333–373.
12. Tonga GY; Moyano DF; Kim CS; Rotello VM, Inorganic nanoparticles for therapeutic delivery: Trials, tribulations and promise. Current Opinion in Colloid & Interface science 2014, 19 (2), 49–55. [PubMed: 24955019]
13. Anselmo AC; Mitragotri S, A review of clinical translation of inorganic nanoparticles. The AAPS journal 2015, 17 (5), 1041–1054. [PubMed: 25956384]
14. Pu X; Li J; Qiao P; Li M; Wang H; Zong L; Yuan Q; Duan S, Mesoporous Silica nanoparticles as a prospective and promising approach for drug delivery and biomedical applications. Current cancer drug targets 2019, 19 (4), 285–295. [PubMed: 30520373]
15. Khurana A; Tekula S; Saifi MA; Venkatesh P; Godugu C, Therapeutic applications of selenium nanoparticles. Biomedicine & Pharmacotherapy 2019, 111, 802–812. [PubMed: 30616079]
16. de Jesus P. d. C. C; Pellosi DS.; Tedesco AC, Magnetic nanoparticles: applications in biomedical processes as synergic drug-delivery systems In Materials for Biomedical Engineering, Elsevier: 2019; pp 365–390.
17. Mohammadpour R; Dobrovolskaia MA; Cheney DL; Greish KF; Ghandehari H, Subchronic and chronic toxicity evaluation of inorganic nanoparticles for delivery applications. Advanced drug delivery reviews 2019, 144, 112–132. [PubMed: 31295521]
18. Oberdorster G, Significance of particle parameters in the evaluation of exposure-doseresponse relationships of inhaled particles. Inhalation toxicology 1996, 8, 73–89. [PubMed: 11542496]
19. Park E-J; Bae E; Yi J; Kim Y; Choi K; Lee SH; Yoon J; Lee BC; Park K, Repeated-dose toxicity and inflammatory responses in mice by oral administration of silver nanoparticles. Environmental toxicology and pharmacology 2010, 30 (2), 162–168. [PubMed: 21787647]

20. Park E-J; Kim H; Kim Y; Yi J; Choi K; Park K, Inflammatory responses may be induced by a single intratracheal instillation of iron nanoparticles in mice. Toxicology 2010, 275 (1–3), 65–71. [PubMed: 20540983]
21. Park E-J; Yoon J; Choi K; Yi J; Park K, Induction of chronic inflammation in mice treated with titanium dioxide nanoparticles by intratracheal instillation. Toxicology 2009, 260 (1–3), 37–46. [PubMed: 19464567]
22. van der Zande M; Vandebriel RJ; Groot MJ; Kramer E; Rivera ZEH; Rasmussen K; Ossenkoppele JS; Tromp P; Gremmer ER; Peters RJ, Subchronic toxicity study in rats orally exposed to nanostructured silica. Particle and fibre toxicology 2014, 11 (1), 8. [PubMed: 24507464]
23. Cho W-S; Duffin R; Poland CA; Howie SE; MacNee W; Bradley M; Megson IL; Donaldson K, Metal oxide nanoparticles induce unique inflammatory footprints in the lung: important implications for nanoparticle testing. Environmental health perspectives 2010, 118 (12), 1699–1706. [PubMed: 20729176]
24. De Jong WH; Van Der Ven LT; Sleijffers A; Park MV; Jansen EH; Van Loveren H; Vandebriel RJ, Systemic and immunotoxicity of silver nanoparticles in an intravenous 28 days repeated dose toxicity study in rats. Biomaterials 2013, 34 (33), 8333–8343. [PubMed: 23886731]
25. Ji JH; Jung JH; Kim SS; Yoon J-U; Park JD; Choi BS; Chung YH; Kwon IH; Jeong J; Han BS, Twenty-eight-day inhalation toxicity study of silver nanoparticles in Sprague-Dawley rats. Inhalation toxicology 2007, 19 (10), 857–871. [PubMed: 17687717]
26. Yun JW; Kim SH; You JR; Kim WH; Jang JJ; Min SK; Kim HC; Chung DH; Jeong J; Kang BC, Comparative toxicity of silicon dioxide, silver and iron oxide nanoparticles after repeated oral administration to rats. Journal of Applied Toxicology 2015, 35 (6), 681–693. [PubMed: 25752675]
27. Garcia T; Lafuente D; Blanco J; Sánchez DJ; Sirvent JJ; Domingo JL; Gómez M, Oral subchronic exposure to silver nanoparticles in rats. Food and Chemical Toxicology 2016, 92, 177–187. [PubMed: 27090107]
28. Valko M; Morris H; Cronin M, Metals, toxicity and oxidative stress. Current medicinal chemistry 2005, 12 (10), 1161–1208. [PubMed: 15892631]
29. Program NT, 11th report on carcinogens. US Department of Health and Human Services 2005.
30. Kwon S; Singh RK; Perez RA; Abou Neel EA; Kim H-W; Chrzanowski W, Silica-based mesoporous nanoparticles for controlled drug delivery. Journal of tissue engineering 2013, 4, 2041731413503357. [PubMed: 24020012]
31. Chen F; Hableel G; Zhao ER; Jokerst JV, Multifunctional nanomedicine with silica: Role of silica in nanoparticles for theranostic, imaging, and drug monitoring. Journal of colloid and interface science 2018, 521, 261–279. [PubMed: 29510868]
32. Center MSKC, A first in human study using 89Zr-cRGDY ultrasmall silica particle tracers for malignant brain tumors. ClinicalTrials.gov Identifier: NCT03465618.
33. Center MSKC, Targeted Silica nanoparticles for real-time image-guided intraoperative mapping of nodal Metastases. ClinicalTrials.gov Identifier: NCT02106598.
34. Noha Ayman Ghallab CU, Evaluation of nano-crystalline hydroxyapatite silica gel in management of periodontal intrabony defects. ClinicalTrials.gov Identifier: NCT02507596.
35. LLC OK, Efficacy of the administration of colloidal silicon dioxide in tablet dosage form in patients with acute diarrhea. ClinicalTrials.gov Identifier: NCT03633344.
36. Liu T; Li L; Teng X; Huang X; Liu H; Chen D; Ren J; He J; Tang F, Single and repeated dose toxicity of mesoporous hollow silica nanoparticles in intravenously exposed mice. Biomaterials 2011, 32 (6), 1657–1668. [PubMed: 21093905]
37. Yu T; Hubbard D; Ray A; Ghandehari H, In vivo biodistribution and pharmacokinetics of silica nanoparticles as a function of geometry, porosity and surface characteristics. Journal of controlled release 2012, 163 (1), 46–54. [PubMed: 22684119]
38. Greish K; Thiagarajan G; Herd H; Price R; Bauer H; Hubbard D; Burckle A; Sadekar S; Yu T; Anwar A, Size and surface charge significantly influence the toxicity of silica and dendritic nanoparticles. Nanotoxicology 2012, 6 (7), 713–723. [PubMed: 21793770]
39. Chan W-T; Liu C-C; Chiau J-SC; Tsai S-T; Liang C-K; Cheng M-L; Lee H-C; Yeung C-Y; Hou S-Y, In vivo toxicologic study of larger silica nanoparticles in mice. International journal of nanomedicine 2017, 12, 3421. [PubMed: 28496319]

40. Malugin A; Ghandehari H, Caspase 3 independent cell death induced by amorphous silica nanoparticles. Nanoscience and Nanotechnology Letters 2011, 3 (3), 309–313.
41. Yu Y; Zhu T; Li Y; Jing L; Yang M; Li Y; Duan J; Sun Z, Repeated intravenous administration of silica nanoparticles induces pulmonary inflammation and collagen accumulation via JAK2/STAT3 and TGF-β/Smad3 pathways in vivo. International Journal of Nanomedicine 2019, 14, 7237. [PubMed: 31564876]
42. Weaver JL; Tobin GA; Ingle T; Bancos S; Stevens D; Rouse R; Howard KE; Goodwin D; Knapton A; Li X, Evaluating the potential of gold, silver, and silica nanoparticles to saturate mononuclear phagocytic system tissues under repeat dosing conditions. Particle and fibre toxicology 2017, 14 (1), 25. [PubMed: 28716104]
43. Ivanov S; Zhuravsky S; Yukina G; Tomson V; Korolev D; Galagudza M, In vivo toxicity of intravenously administered silica and silicon nanoparticles. Materials 2012, 5 (10), 1873–1889.
44. Lee S; Kim M-S; Lee D; Kwon TK; Khang D; Yun H-S; Kim S-H, The comparative immunotoxicity of mesoporous silica nanoparticles and colloidal silica nanoparticles in mice. International journal of nanomedicine 2013, 8, 147. [PubMed: 23326190]
45. Tamion A; Hillenkamp M; Hillion A; Maraloiu VA; Vlaicu ID; Stefan M; Ghica D; Rositi H; Chauveau F; Blanchin M-G, Ferritin surplus in mouse spleen 14 months after intravenous injection of iron oxide nanoparticles at clinical dose. Nano Research 2016, 9 (8), 2398–2410.
46. Kolosnjaj-Tabi J; Javed Y; Lartigue L; Volatron J; Elgrabli D; Marangon I; Pugliese G; Caron B; Figuerola A; Luciani N, The one year fate of iron oxide coated gold nanoparticles in mice. ACS nano 2015, 9 (8), 7925–7939. [PubMed: 26168364]
47. Saikia J; Yazdimamaghani M; Hadipour Moghaddam SP; Ghandehari H, Differential protein adsorption and cellular uptake of silica nanoparticles based on size and porosity. ACS applied materials & interfaces 2016, 8 (50), 34820–34832. [PubMed: 27998138]
48. Moghaddam SPH; Mohammadpour R; Ghandehari H, In vitro and in vivo evaluation of degradation, toxicity, biodistribution, and clearance of silica nanoparticles as a function of size, porosity, density, and composition. Journal of Controlled Release 2019, 311, 1–15. [PubMed: 31465825]
49. Yu T; Malugin A; Ghandehari H, Impact of silica nanoparticle design on cellular toxicity and hemolytic activity. ACS nano 2011, 5 (7), 5717–5728. [PubMed: 21630682]
50. Herd HL; Malugin A; Ghandehari H, Silica nanoconstruct cellular toleration threshold in vitro. Journal of controlled release 2011, 153 (1), 40–48. [PubMed: 21342660]
51. Malugin A; Herd H; Ghandehari H, Differential toxicity of amorphous silica nanoparticles toward phagocytic and epithelial cells. Journal of Nanoparticle Research 2011, 13 (10), 5381.
52. Yazdimamaghani M; Moos PJ; Ghandehari H, Global gene expression analysis of macrophage response induced by nonporous and porous silica nanoparticles. Nanomedicine: Nanotechnology, Biology and Medicine 2018, 14 (2), 533–545.
53. Yazdimamaghani M; Moos PJ; Ghandehari H, Time-and dose-dependent gene expression analysis of macrophage response as a function of porosity of silica nanoparticles. Nanomedicine: Nanotechnology, Biology and Medicine 2019, 21, 102041.
54. D'Mello SR; Cruz CN; Chen M-L; Kapoor M; Lee SL; Tyner KM, The evolving landscape of drug products containing nanomaterials in the United States. Nature nanotechnology 2017, 12 (6), 523.
55. de la Harpe KM; Kondiah PP; Choonara YE; Marimuthu T; du Toit LC; Pillay V, The hemocompatibility of nanoparticles: a review of cell–nanoparticle interactions and hemostasis. Cells 2019, 8 (10), 1209.
56. Neun BW; Ilinskaya AN; Dobrovolskaia MA, Analysis of complement activation by nanoparticles In Characterization of Nanoparticles Intended for Drug Delivery, Springer: 2018; pp 149–160.
57. Dobrovolskaia MA; McNeil SE, Understanding the correlation between in vitro and in vivo immunotoxicity tests for nanomedicines. Journal of controlled release 2013, 172 (2), 456–466. [PubMed: 23742883]
58. Dobrovolskaia MA; Clogston JD; Neun BW; Hall JB; Patri AK; McNeil SE, Method for analysis of nanoparticle hemolytic properties in vitro. Nano letters 2008, 8 (8), 2180–2187. [PubMed: 18605701]

59. Neun BW; Dobrovolskaia MA, Method for analysis of nanoparticle hemolytic properties in vitro In Characterization of nanoparticles intended for drug delivery, Springer: 2011; pp 215–224.
60. Killick J; Morisse G; Sieger D; Astier AL In Complement as a regulator of adaptive immunity, Seminars in immunopathology, Springer: 2018; pp 37–48.
61. Szebeni J, Complement activation-related pseudoallergy: a stress reaction in blood triggered by nanomedicines and biologicals. Molecular immunology 2014, 61 (2), 163173.
62. Burkholder T; Foltz C; Karlsson E; Linton CG; Smith JM, Health evaluation of experimental laboratory mice. Current protocols in mouse biology 2012, 2 (2), 145–165. [PubMed: 22822473]
63. Kalueff A; Minasyan A; Keisala T; Shah Z; Tuohimaa P, Hair barbering in mice: implications for neurobehavioural research. Behavioural processes 2006, 71 (1), 8–15. [PubMed: 16236465]
64. Brodkin ES, BALB/c mice: low sociability and other phenotypes that may be relevant to autism. Behavioural brain research 2007, 176 (1), 53–65. [PubMed: 16890300]
65. Demer LL; Tintut Y, Inflammatory, metabolic, and genetic mechanisms of vascular calcification. Arteriosclerosis, thrombosis, and vascular biology 2014, 34 (4), 715–723.
66. Karwowski W; Naumnik B; Szczepański M; Myśliwiec M, The mechanism of vascular calcification–a systematic review. Medical science monitor: international medical journal of experimental and clinical research 2012, 18 (1), RA1. [PubMed: 22207127]
67. Liu Y; Shanahan CM, Signalling pathways and vascular calcification. Front Biosci 2011, 16 (1302), 14.
68. Zhang Y-N; Poon W; Tavares AJ; McGilvray ID; Chan WC, Nanoparticle–liver interactions: Cellular uptake and hepatobiliary elimination. Journal of controlled release 2016, 240, 332–348. [PubMed: 26774224]
69. Stravitz RT; Sanyal AJ, Drug-induced steatohepatitis. Clinics in liver disease 2003, 7 (2), 435–451. [PubMed: 12879993]
70. Brunt EM, Pathology of fatty liver disease. Modern Pathology 2007, 20 (1s), S40. [PubMed: 17486051]
71. Liss KH; McCommis KS; Chambers KT; Pietka TA; Schweitzer GG; Park SL; Nalbantoglu I; Weinheimer CJ; Hall AM; Finck BN, The impact of diet-induced hepatic steatosis in a murine model of hepatic ischemia/reperfusion injury. Liver Transplantation 2018, 24 (7), 908–921. [PubMed: 29729104]
72. Möller K; Bein T, Degradable drug carriers: vanishing mesoporous silica nanoparticles. Chemistry of Materials 2019, 31 (12), 4364–4378.
73. Dobrovolskaia MA; Germolec DR; Weaver JL, Evaluation of nanoparticle immunotoxicity. Nature nanotechnology 2009, 4 (7), 411.
74. Salvador-Morales C; Flahaut E; Sim E; Sloan J; Green ML; Sim RB, Complement activation and protein adsorption by carbon nanotubes. Molecular immunology 2006, 43 (3), 193–201. [PubMed: 16199256]
75. Chen F; Wang G; Griffin JI; Brenneman B; Banda NK; Holers VM; Backos DS; Wu L; Moghimi SM; Simberg D, Complement proteins bind to nanoparticle protein corona and undergo dynamic exchange in vivo. Nature nanotechnology 2017, 12 (4), 387.
76. Ilinskaya AN; Shah A; Enciso AE; Chan KC; Kaczmarczyk JA; Blonder J; Simanek EE; Dobrovolskaia MA, Nanoparticle physicochemical properties determine the activation of intracellular complement. Nanomedicine: Nanotechnology, Biology and Medicine 2019, 17, 266–275.
77. Wang G; Chen F; Banda NK; Holers VM; Wu L; Moghimi SM; Simberg D, Activation of human complement system by dextran-coated iron oxide nanoparticles is not affected by dextran/Fe ratio, hydroxyl modifications, and crosslinking. Frontiers in immunology 2016, 7, 418. [PubMed: 27777575]
78. Tenzer S; Docter D; Rosfa S; Wlodarski A; Kuharev J r.; Rekik, A.; Knauer, S. K.; Bantz, C.; Nawroth, T.; Bier, C., Nanoparticle size is a critical physicochemical determinant of the human blood plasma corona: a comprehensive quantitative proteomic analysis. ACS nano 2011, 5 (9), 7155–7167. [PubMed: 21866933]

79. Nishimori H; Kondoh M; Isoda K; Tsunoda S-i.; Tsutsumi, Y.; Yagi, K., Silica nanoparticles as hepatotoxicants. European Journal of Pharmaceutics and Biopharmaceutics 2009, 72 (3), 496–501. [PubMed: 19232391]

80. Xie G; Sun J; Zhong G; Shi L; Zhang D, Biodistribution and toxicity of intravenously administered silica nanoparticles in mice. Archives of toxicology 2010, 84 (3), 183–190. [PubMed: 19936708]

81. Kim SY; Meyer HW; Saalwächter K; Zukoski CF, Polymer dynamics in PEGsilica nanocomposites: Effects of polymer molecular weight, temperature and solvent dilution. Macromolecules 2012, 45 (10), 4225–4237.

82. Shen S; Wu Y; Liu Y; Wu D, High drug-loading nanomedicines: progress, current status, and prospects. International journal of nanomedicine 2017, 12, 4085. [PubMed: 28615938]

83. Shen J; He Q; Gao Y; Shi J; Li Y, Mesoporous silica nanoparticles loading doxorubicin reverse multidrug resistance: performance and mechanism. Nanoscale 2011, 3 (10), 4314–4322. [PubMed: 21892492]

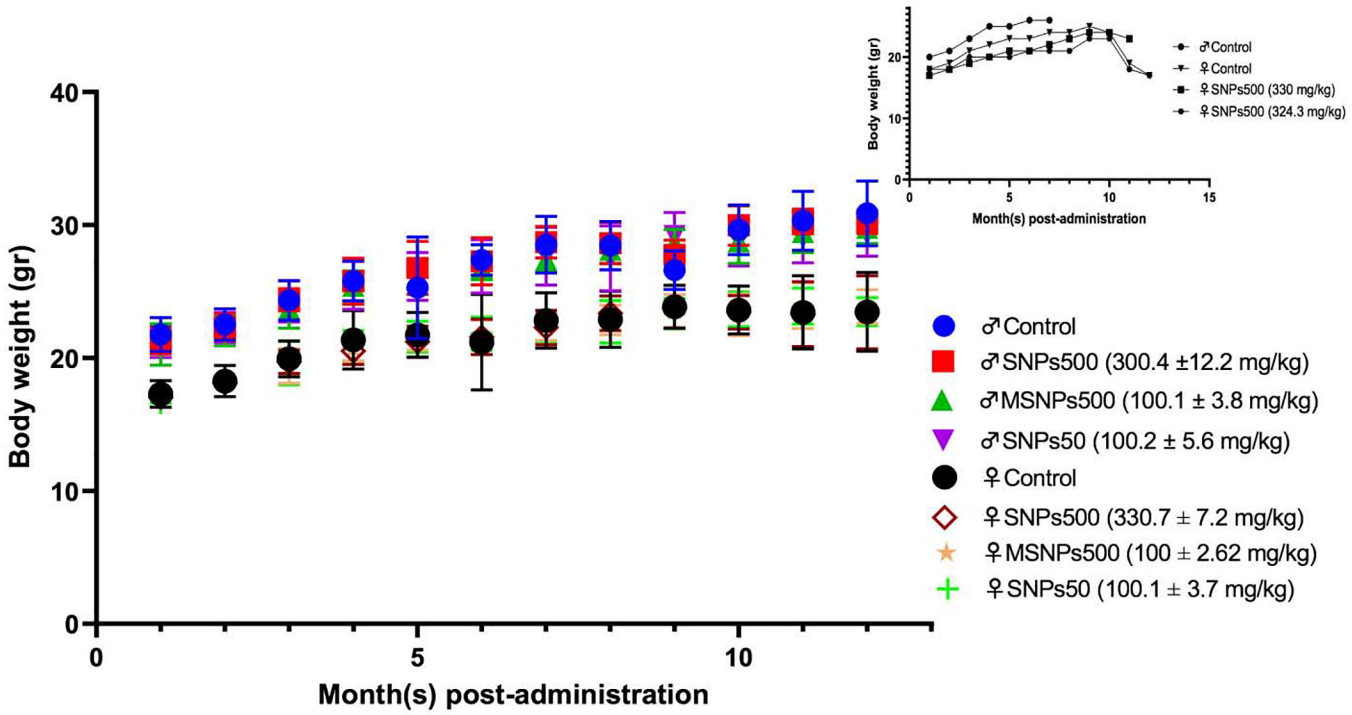


**Figure 1.**

Body weight changes of BALB/c mice over one-year post IV administration of various SNPs at indicated doses. The increasing body weight rate of injected female and male BALB/c mice was the same as relevant sex of saline injected control groups. *Inset:* Body weight changes of dead mice during one year. Four out of 80 animals died during the one-year study two of which were saline injected mice (female and male) and two were females that received large Stöber silica nanoparticles (SNPs500).

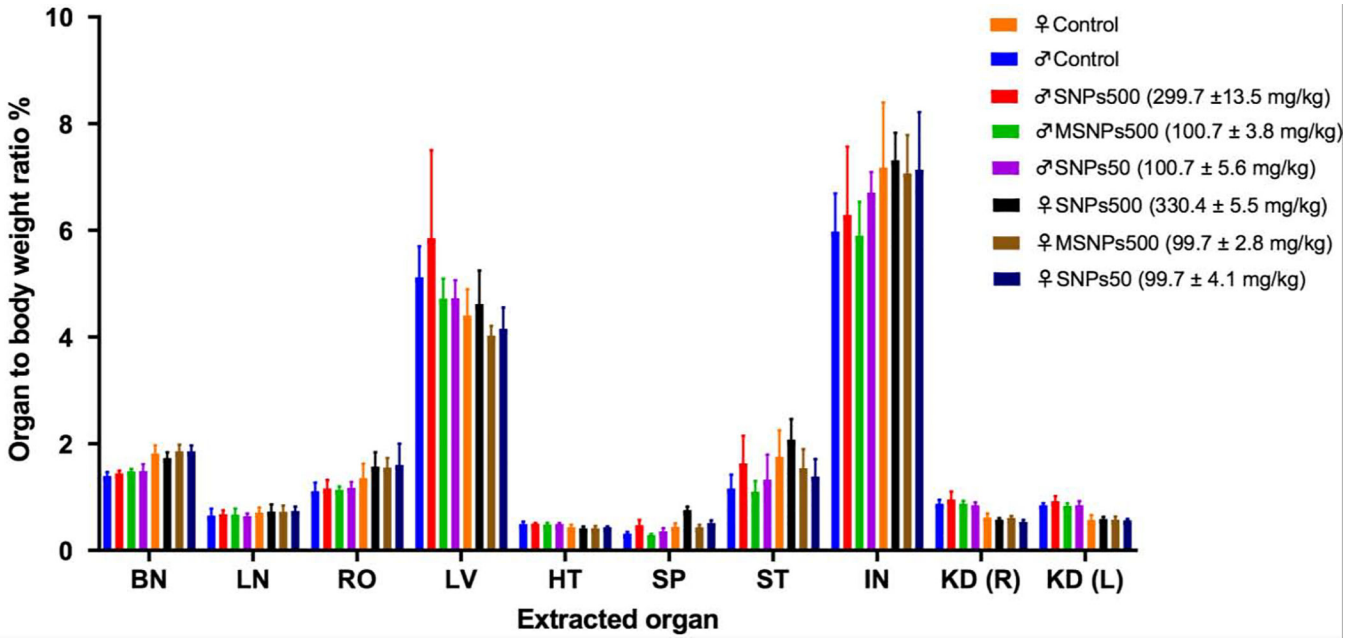


**Figure 2.**

Normalized organ-to-body weight ratio percentages of female and male BALB/c mice that were administered intravenously with different silica NPs and survived for a year. Significant differences in organ-to-body weight ratio percentages between nanoparticle treated groups and control groups were not observed. Abbreviations: brain (BN), lung (LN), reproductive organs (RO), heart (HT), spleen (SP), stomach (ST), intestine (IN), kidney (KD) right (R) and left (L).

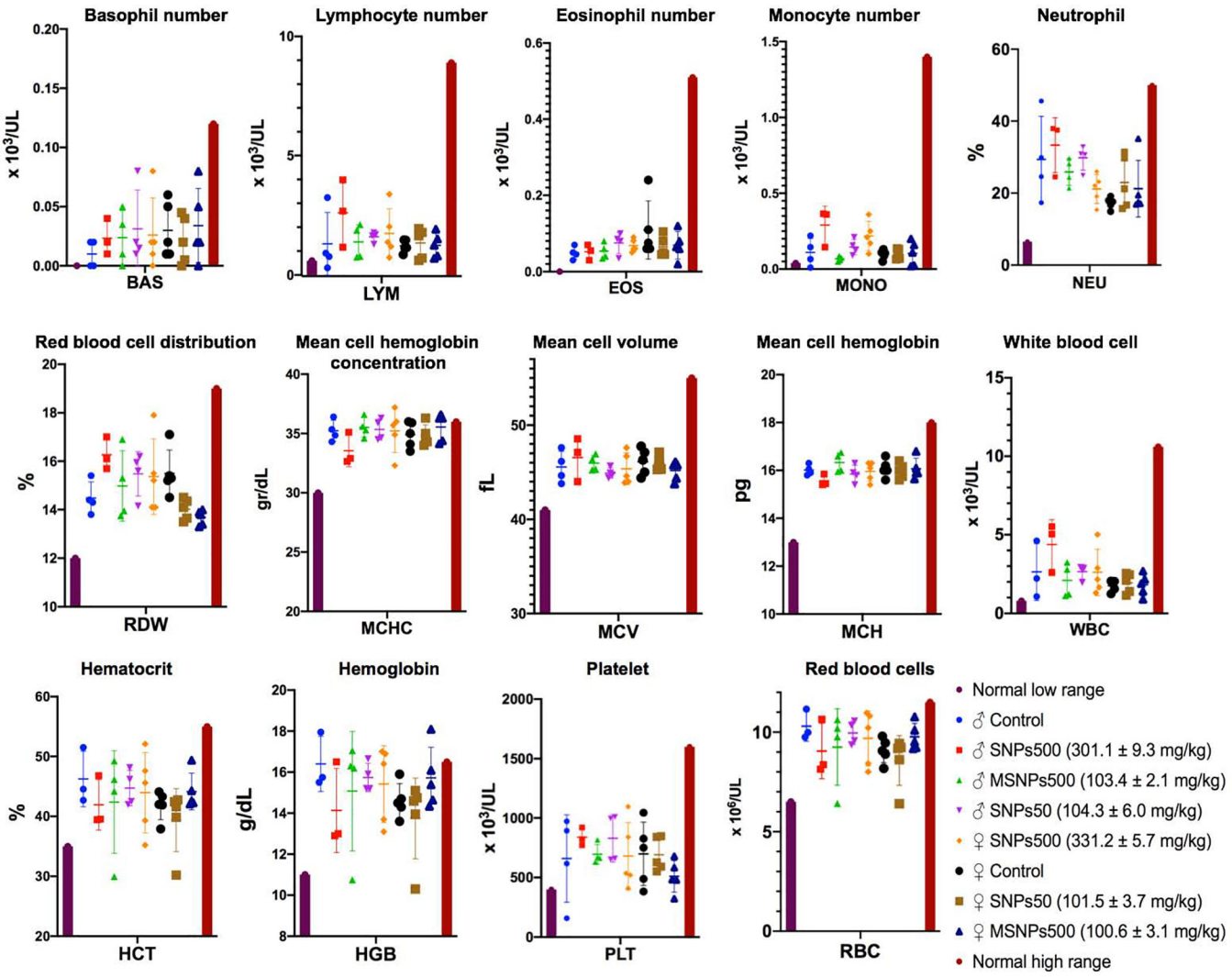


**Figure 3.**

Hematological values of female and male BALB/c mice injected with various SNPs at indicated doses. The first and last columns are the minimum and maximum average normal range in both sexes. Significant blood level changes were not observed in any of the cohorts studied.

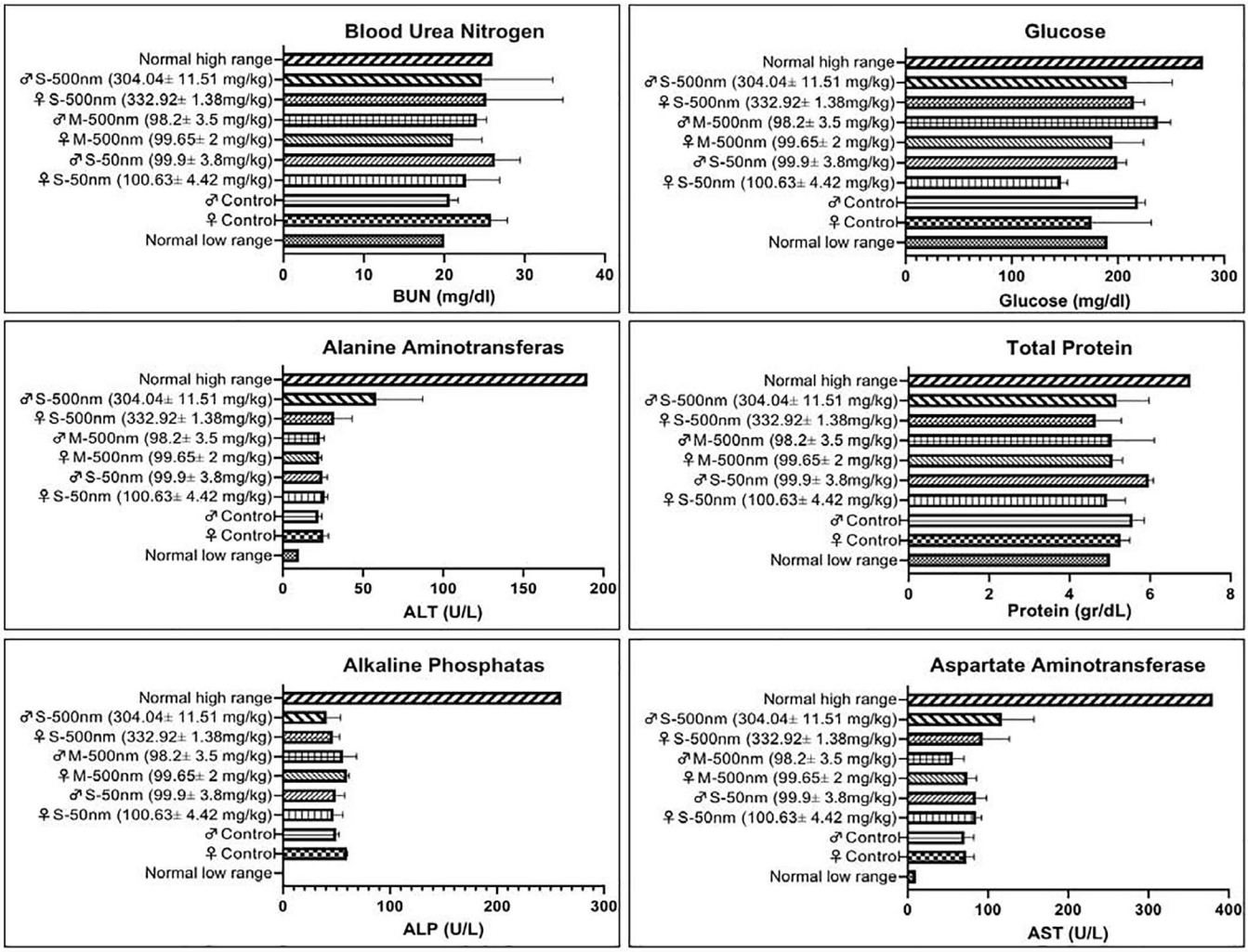


**Figure 4.**

Plasma biochemistry values of surviving one-year mice administered SNPs intravenously at indicated doses. The results show there is no significant difference in alanine aminotransferase (ALT), aspartate amino transferase (AST), alkaline phosphatase (ALP), blood urea nitrogen (BUN) total protein, and glucose of treated animals.

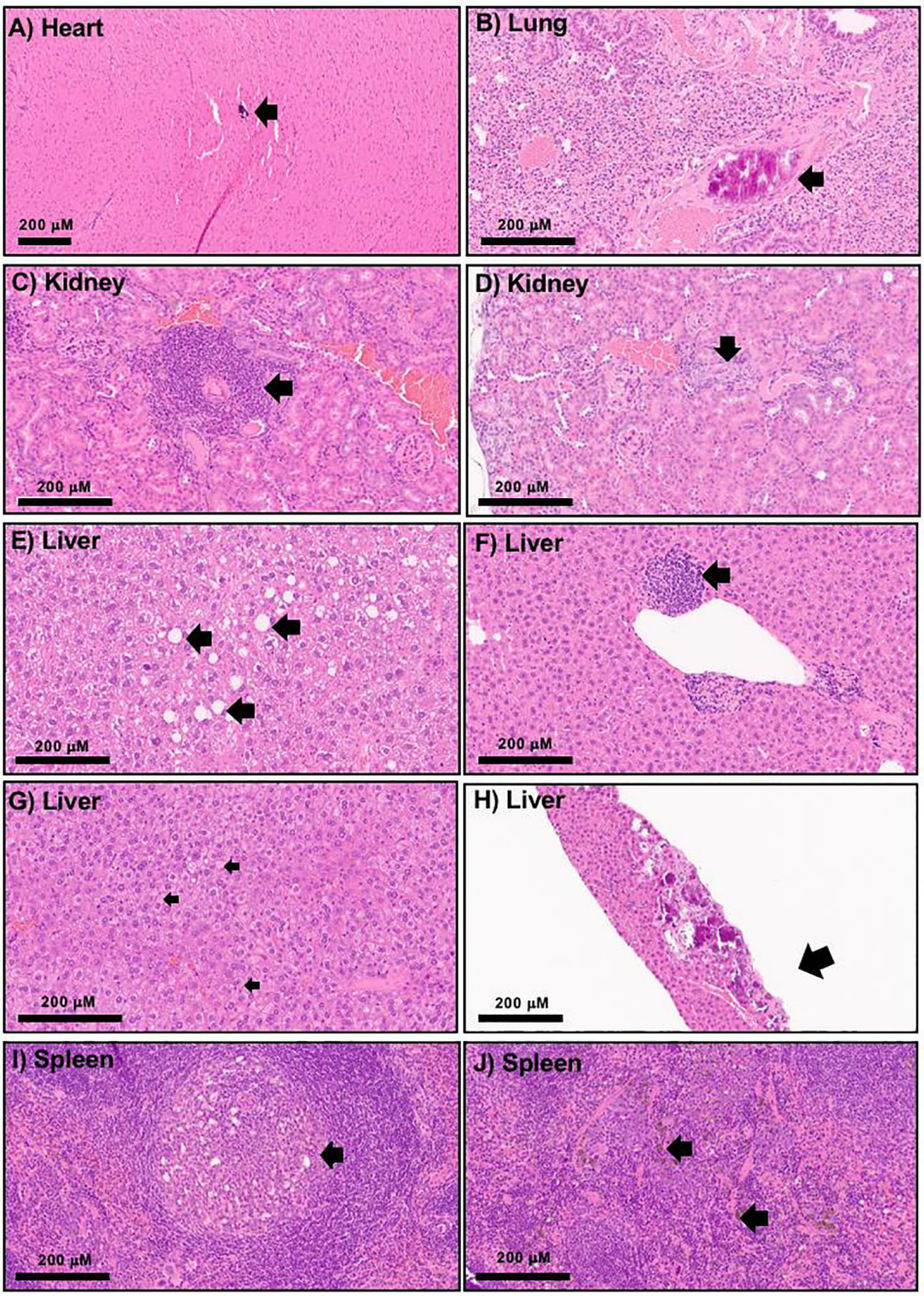


**Figure 5.**

20x H and E microscopic images of histologic changes one-year post SNPs IV injection (A-F and H-J) identified in various organs including focal myocardial calcification(s), likely intravascular (A), calcification within the pulmonary vessels (B), focal lymphocytic infiltrate within the renal interstitium (C), focal white blood cell casts in renal tubule (D), minimal to mild macrovesicular steatosis, without ballooning or Mallory hyaline (E), focal inflammation within the liver tissue mostly composed of lymphocytes with admixed pigment laden macrophages (F), marked microvesicular steatosis in one of the control animals (G),

liver tissue with subcapsular fibrosis and calcifications (H), aggregates of histocytes and neutrophils within the white pulp (I), and splenic hemosiderin deposition (J).

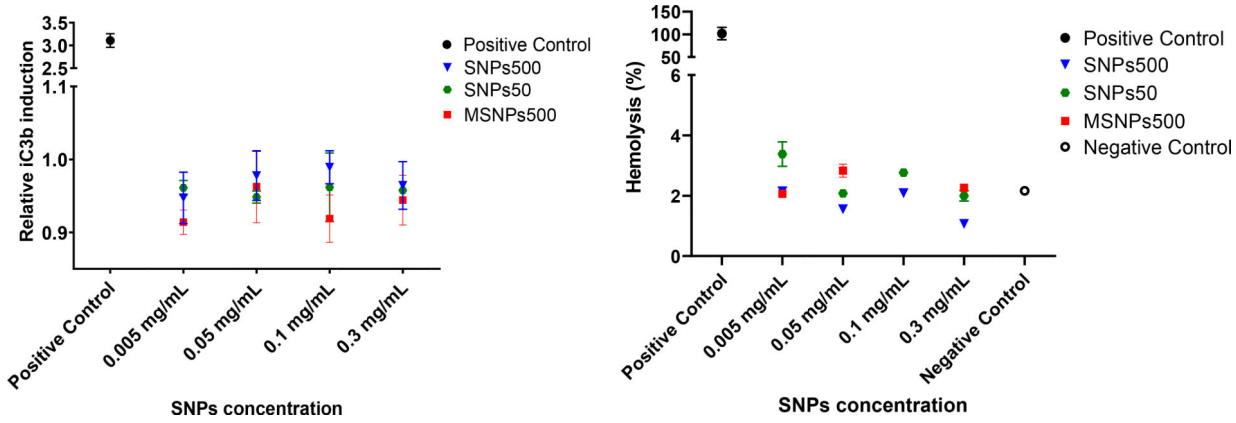


**Figure 6.**

a) Relative iC3b concentration in human plasma incubated with SNPs50, SNP500 and MSNPs500 to saline control. Data plotted as mean ± standard deviation of three repeats. b) Percent hemolysis of human blood following 3 hours incubation with SNPs50, SNPs500 and MSNPs500.

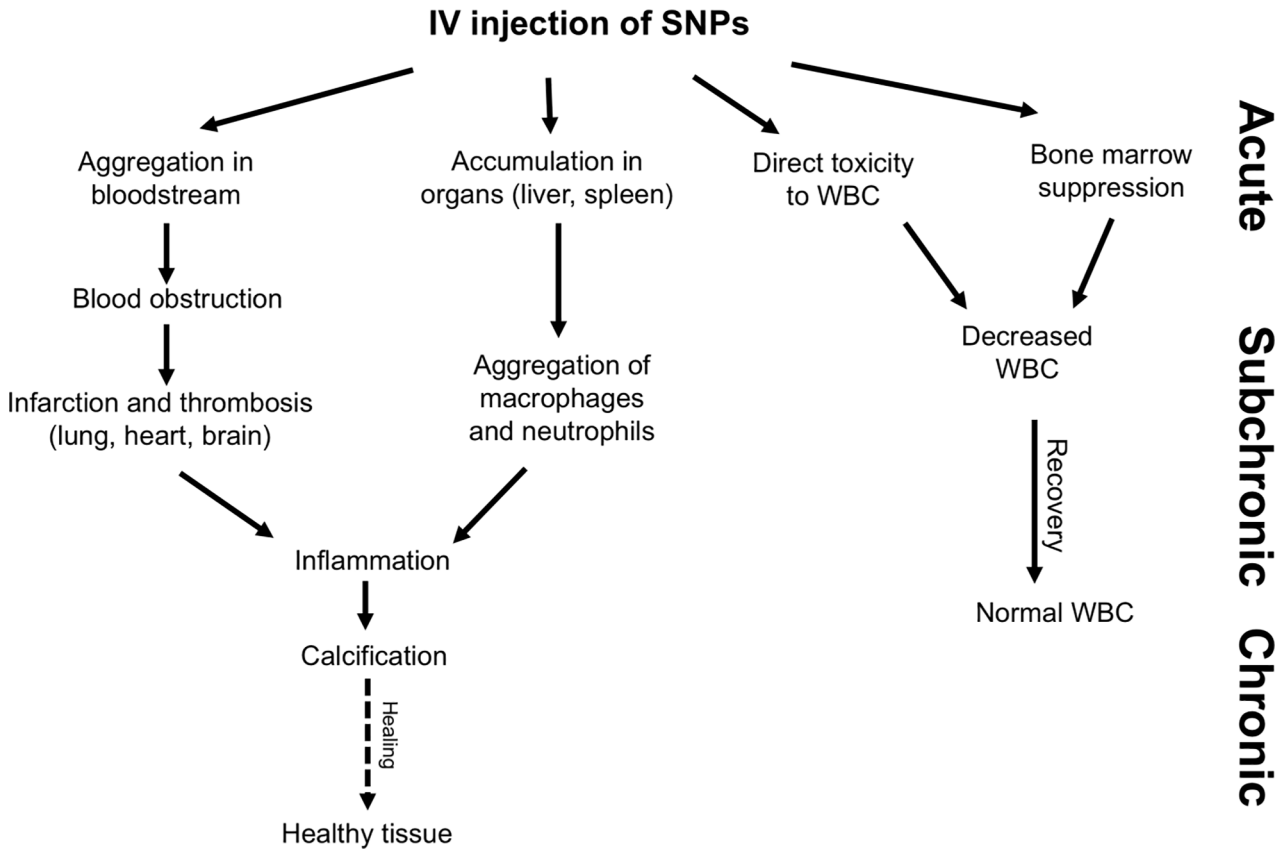


**Figure 7.**

Possible healing outcomes induced by silica NPs during acute, subchronic and chronic evaluation following single dose intravenous administration.